

Coupled Field Problems

Edited by

A. Kassab

University of Central Florida, USA

M.H. Aliabadi

Queen Mary, University of London, UK

WITPRESS Southampton, Boston



Contents

Preface	ix
Chapter 1	
Using BEM in glass modelling	
R.M.M. Matheij, H.G. ter Morsche and K. Wang	1
Chapter 2	
Interaction of radiation with other heat transfer modes	
R.A. Bialecki, E. Grela and G. Węcel	39
Chapter 3	
Coupled FVM/BEM approach to conjugate heat transfer	
A. Kassab, H. Li and Y. Ren	79
Chapter 4	
Boundary element method, sensitivity analysis and conjugate problems	
C.L. Chan	105
Chapter 5	
Aero-thermo-elastic concurrent design optimization of internally cooled turbine blades	
T.J. Martin and G.S. Dulikravich	137
Chapter 6	
Dual boundary element formulations for steady state and transient thermoelastic fracture mechanics	
M.H. Aliabadi	185
Chapter 7	
Poroelasticity using the BEM	
M. Chopra	211

image to
or

transmitted
without the

Chapter 5

Aero-thermo-elastic concurrent design optimization of internally cooled turbine blades

T. J. Martin & G. S. Dulikravich

*Multidisciplinary Analysis, Inverse Design, and Optimization Lab.
Department of Mechanical and Aerospace Engineering, Box 19018
University of Texas, Arlington, USA.*

Abstract

This text presents the theoretical methodology, organizational strategy and application of a fully automated computer program for the multi-disciplinary design, optimization and virtual prototyping of internally cooled axial gas turbine airfoils. A three-dimensional cooled turbine airfoil generation program was written to provide automatic transfer of geometric and boundary condition information from the engine cycle, aero-thermal, heat conduction, thermo-fluid and thermo-elastic analysis programs. The set of optimization design variables defined the geometry, internal coolant passage configuration, internal heat transfer enhancements, coolant supply pressures and turbine inlet temperature. A constrained optimization algorithm was used to control the thermal optimization process to maximize the cooling effectiveness or engine specific thrust subject to material integrity and durability constraints. The constrained optimization problems required 300-800 objective and constraint function analyses. The boundary element method (BEM) was used to solve the non-linear heat conduction equation iteratively coupled to a computational fluid dynamics (CFD) code for the conjugate prediction of the heat transfer between the hot gas and the solid blade. A compressible system of fluid elements was developed for the serpentine coolant network to calculate the pressure losses, flow rate and heat balance between the blade and coolant fluid. The BEM temperature field was analyzed to maintain material integrity and to maximize blade durability against creep and corrosion. A two-dimensional thermo-elastic BEM code was developed for the enforcement of the thermo-mechanical fatigue (TMF) constraint. Implicit differentiation of the thermal and thermo-elastic solvers was performed to compute design sensitivity derivatives faster and more accurately than via explicit finite differencing. A factor of three savings of computer processing time was realized for two-dimensional problems and a factor of twenty was obtained for three-dimensional problems, but the program's memory requirements were doubled. Results have shown that a significant increase in engine performance can be achieved with computer automation of the turbine cooling design optimization process.

1 Introduction

The greatest efficiency improvements in gas turbine engines are likely to be accomplished by increasing the rotor speed and turbine inlet temperature. Higher rotor speeds can contribute directly to higher thrust-to-weight ratios and more compact engines by allowing more power to be extracted from each turbine stage. Unfortunately, the maximum centrifugal loads in the rotor blade generally set the angular speed limit for a given tip radius of a blade that is to be manufactured from a given type of material. Although it is desirable to maximize the turbine blade's durability by minimizing cycle fatigue, this type of thermo-structural optimization is beyond the scope of this research for other reasons. First, the quantification of the engine performance with respect to the rotor speed is intrinsically related to a rigorous modeling of the compressor. Second, highly non-linear aero-elastic modeling, being necessary to predict fatigue life limited by vibratory stresses, is prohibitively expensive for computational automation. On the other hand, the practical benefits of computer automated maximization of the temperature while maintaining material integrity can be done with fewer resources and with more reliable and existing software codes.

The advantages of increasing the turbine inlet temperature can be demonstrated by examining its effect on a standard engine performance parameter, such as specific thrust. Due to the increased amount of energy released by combustion, the specific thrust increases continuously with an increase in the turbine inlet temperature for all engine classifications, assuming that all other variables such as flight Mach number and air mass flow rate are held constant (Lakshminarayana [1]). The thrust-specific fuel consumption is another performance parameter which is important for civil transport aircraft engines, that is, fuel economy. The proportionality of temperature to specific fuel consumption is a little more complicated because higher temperature drops allow larger amounts of power to be extracted by the turbine. Given that each compressor stage is designed at its operational limit as defined by the maximum stall pressure ratio, the optimum compressor pressure ratio is dependent upon that available power. Ultimately, increasing the turbine inlet temperature has a favorable effect on fuel economy. In addition, greater temperature drops per stage can lead directly to more compact engines. Thus, increasing the turbine inlet temperature optimizes all engine performance parameters such as specific thrust, thrust-specific fuel consumption and engine weight. Typically, a 1% increase in turbine inlet temperature can produce a 3% to 4% increase in engine output (Hill & Peterson [2]; Brown et al. [3]).

There is an obvious thermal limit in the turbine because of melting, oxidation and sulfidation (hot corrosion) of the blades, not to mention that the increased temperature environment in the presence of high centrifugal and bending loads increases the stresses, adversely affects the blade life due to thermally-enhanced creep, thermo-mechanical fatigue caused by cyclic stress and high temperature gradients that induce cracking, thermal barrier coating delamination and plastic thermal strains. Thus, the temperature in the turbine has a more broad effect on engine performance. For these reasons, this research has focused only upon the computer-automated aerodynamic and thermal optimization of the turbine with the application of thermal integrity, oxidation life, structural integrity and thermo-mechanical fatigue life constraints at a fixed rotor speed.

1.1 N

A
 D_h
 e_s
 ϵ
 f
 F
 G
 G_{cool}
 γ
 H
 h_{cool}
 h_0
 η
 k
 \dot{m}
 \dot{m}_f
 M
 μ
 ρ
 s
 p_0
 $P_{t,cool}$
 π_c
 Q
 r
 R_K
 σ_{ij}
 t_s
 T
 \bar{T}
 $T_{t,cool}$
 $T_{t,inlet}$
 T_{max}
 T_0
 T_0
 V_i
 w
 W
 Ω
 x_s

1.1 Nomenclature

A	Cross-sectional area of a coolant passage
D_h	Hydraulic diameter of a coolant passage
e_s	Strut fillet radius
ε	Coolant passage wall roughness or trip strip height
f	Friction factor
F	Optimization objective function
G	Inequality constraint function on the optimization
G_{cool}	Mass flow rate of coolant fluid
γ	Ratio of specific heats of an ideal gas
H	Equality constraint function on the optimization
h_{cool}	Heat transfer coefficient on coolant passage walls
h_O	Heat transfer coefficient on outer turbine airfoil surface
η	Cooling effectiveness or convection efficiency
k	Thermal conductivity coefficient
\dot{m}	Air mass flow rate through engine
\dot{m}_f	Mass flow rate of fuel
M	Mach number
μ	Coolant fluid viscosity coefficient
ρ	Density of coolant fluid
s	Turbine airfoil contour following coordinate
p_0	Stagnation pressure
$p_{t,cool}$	Coolant fluid inlet total pressure
π_c	Stagnation pressure ratio across compressor
Q	Heat flux
r	Streamwise (radial) direction of coolant flow
R_K	Coolant pressure loss coefficient in a 180° turning bend
σ_{ij}	Stress tensor
t_s	Strut thickness
T	Temperature
\bar{T}	Average or target temperature
$T_{t,cool}$	Bulk total temperature of coolant
$T_{t,inlet}$	Turbine inlet total temperature
T_{max}	Maximum temperature in turbine blade metal
T_0	Stagnation temperature
T_O	Temperature on outer turbine airfoil surface
V_i	Vector of optimization design variables
w	Coolant fluid average local speed
W	Coolant passage wall thickness
Ω	Engine rotation rate
x_s	Coordinate of strut centerline intersection with turbine airfoil

1.2 Turbine cooling techniques

With presently available materials such as nickel-based alloys, turbine blades cannot withstand metal temperatures in excess of 1300 K. Turbine inlet temperatures of modern engines already exceed this amount, especially for high-speed aircraft, because internal and external cooling of the turbine blades allows those higher gas temperatures. Modern turbomachinery rotor and stator blades have traditionally been cooled by directing compressor bleed air through passages in the engine and into complex serpentine-like coolant flow passages inside the blades (Mochizuki et al. [4]). Much of the cooling is accomplished via convection on the coolant passage surfaces. Typically, the cooling air provides a heat sink that is only 400 to 450 K cooler than the maximum metal temperature. The incorporation of internal cooling and improvements in materials have resulted in increases in turbine inlet gas temperatures from 850 K in the 1960s to 1600 K today, with about 350 K of this increase attributed to the cooling devices alone (Kawaike et al. [5]; Ikeguchi & Kawaike [6]). Internal cooling of turbine blades has been a major focus in modern turbomachinery and manufacturing for over thirty years. For classical blade materials and geometric design it has been effective for turbine inlet gas temperatures up to approximately 1560 K. The more recent external (film) cooling techniques allow even greater inlet gas temperatures of up to 1800 K. Film cooling can produce a protective layer of cool air on the surface of the blades, but more cooling air bled from higher compressor stages are necessary, and they result in greater external pressure losses due to a reduction in the boundary layer momentum. Moreover, with the current efforts to push the inlet turbine gas temperatures even higher, an opposite effect becomes significant. This is the production of NO_x that starts occurring at high temperatures. Consequently, there is renewed interest in exploring the possibilities of better closed-loop high-pressure internal cooling schemes. Because of the computational complexities involved, film cooling was not incorporated into this research, and focus has been exclusively upon internal cooling techniques.

All of the internal cooling techniques involve increased aerodynamic losses and decreased efficiency resulting from the bleeding of air from the compressor. External losses are associated with a loss of power from the coolant flow and increased profile losses due to thicker blades arising from the coolant holes. Generally, the greater the coolant flow rate, the more the blades are cooled, but the result is an even greater pressure loss in the coolant passages. Heat transfer enhancements, such as trip strips or turbulators, impingement cooling, tube banks and miniature heat exchangers, can provide further enhancements to the amount of internal convection heat transfer, but they invariably result in disproportionately more pressure loss. In addition, the pressure losses due to the mixing of the coolant with the external flow results in a steady decrease in the net turbine efficiency as the turbine inlet temperature increases (Brown et al. [3]). After considering the effect on aerodynamic efficiency of film cooling and coolant air ejection, it may even worsen the performance of the engine. Also, when bleeding coolant air from the compressor, if the fuel flow rate to the burner is not reduced accordingly, the turbine inlet temperature will be magnified by the same mechanism that allows the blades to handle those higher temperatures. Thus, the advantages of increasing the turbine inlet temperature by internal cooling are offset by the aerodynamic losses, as well as the mechanical and manufacturing complexities of the internal cooling passages. Despite all these difficulties, a considerable gain in turbine performance may be realized to offset all those penalties. So the question is, how can engineers design and optimize an internal turbine blade cooling system?

Dur
develop
cooling
passage
demon
(Kenno
Dulikra
Martin
three-di
by spec
configu
An opt
passage
specific
shape d
bounda

This
the gec
involve
cooled
that the
perform
example
thicknes
of the b
blade f
manual
is not y
At the
remains
simultar
maintain
costs ar
these q
simultar
(MCAD

1.2 MC

Figure 1
the MC/
informat
UNIX C
algorithm
used sev
values fo
responsi

During the past fourteen years, Dulikravich and his research team of graduate students have developed a fully-automatic computational inverse shape design algorithm that allows a cooling systems designer to determine the numbers, sizes, shapes and locations of coolant flow passages within internally cooled configurations. The methodology was successfully demonstrated on multi-holed two-dimensional turbine airfoils with thermal barrier coatings (Kennon & Dulikravich [7]; Chiang & Dulikravich [8]; Dulikravich & Kosovic [9]; Dulikravich & Martin [10]), single-holed three-dimensional turbine blades (Dulikravich & Martin [11]), scramjet combustor struts (Dulikravich [12]), and hydrogen cooled multi-coated three-dimensional rocket nozzle walls (Martin & Dulikravich [13]). This methodology worked by specifying a desirable variation of heat flux over the external surface of the cooled configuration, in addition to the boundary conditions of a well-posed heat conduction problem. An optimization algorithm was then used to modify iteratively the shapes of the coolant passages in an attempt to minimize the squared sum of the difference between the user-specified and numerically computed heat fluxes on the outer boundary. The inverse thermal shape design process continued until the difference between the computed and over-specified boundary conditions converged to a user-specified tolerance.

This inverse thermal shape design methodology worked, but in view of the complexities of the geometry, the intricately coupled engine components and the numerous parameters involved in a turbine, the efficacy of the method fell short of the real objectives of internally cooled turbine blade design. Designers of high-performance jet engines have long recognized that the final design of a turbine blade must represent a compromise among aerodynamic performance, cooling effectiveness, structural integrity, durability and manufacturability. For example, improvements in aero-thermodynamic performance can be realized by reducing blade thickness, but eventually a hard structural design constraint is reached. Either the fatigue life of the blade becomes unacceptably low because of excessive flow-induced vibrations, or the blade flutters with immediate destructive consequences (Bendiksen [14]). Even with the manual design process currently operating in the turbomachinery industry, a systematic method is not yet available for full understanding of cooled turbine efficiency (Lakshminarayana [1]). At the present time, testing is the only reliable method. Thus, the following question still remains, "Is it possible to design manufacturable turbine cooling configurations that simultaneously increase the turbine inlet temperature, decrease the coolant requirements, maintain material integrity and improve airfoil durability, so that engine capital and operating costs are reduced?" This research presents a methodology that proposes to answer some of these questions, and addresses as many of these goals and constraints as possible simultaneously by using our multidisciplinary computer automated design optimization (MCADO).

1.2 MCADO system for internally cooled turbine blades

Figure 1 illustrates how information flows among the main computational components within the MCADO system for internally cooled turbine blades. Boundary condition and parameter information is fed either iteratively or non-iteratively between FORTRAN subroutines using UNIX C-shell scripts, common blocks and argument lists. The constrained optimization algorithm, called OPTRAN, is the main driver program for the MCADO system. OPTRAN used several popular numerical optimization packages to minimize the objective function values for a population of design vectors subject to a finite number of constraint functions. It is responsible for perturbations to the design vector using information received from the

numerical analysis and design programs. This hybrid constrained optimization package was discussed in a recent publication involving genetic and evolutionary optimization algorithms (Dulikravich et al. [15, 16, 17, 18, 19]).

The design variable set defines the geometry of the turbine blade including the external turbine airfoil shape definition, thermal barrier coating thickness, blade wall thickness distribution and blade internal strut configurations. The blade stacking axis, twist and taper are incorporated into the design variable set for three-dimensional blades. Other design variables that do not affect the geometry, such as the turbine inlet temperature, coolant mass flow rate and heat transfer enhancements such as trip strip height, transverse rib spacing and tube bank diameter, are also shown in Figure 1. With a constrained optimization algorithm, the internally cooled turbine blade designs were modified so that the turbine cooling network can handle sequential increases in the turbine inlet temperature with an appropriate amount of coolant air bleed and internal heat transfer enhancement (Martin et al. [20]).

Various aerodynamic and thermal objective functions were attempted with the MCADO system. The objective of the optimization process, shown in the upper-right-hand corner of Figure 1, was quantified as a single scalar function. The aerodynamic objective functions used the CFD-calculated pressure and temperature fields. The thermal objective function used only the calculated temperature field in the turbine blades. In more recent efforts, a fluid element system simulated the internal coolant flow and an engine cycle analysis determined the impact of the design variables on the real engine efficiency so that either the engine specific thrust or thrust-specific fuel consumption was optimized. That engine cycle program requested information about the engine operating conditions, such as flight Mach number, altitude, air intake, rotor speed and component efficiencies (inlet, compressor, burner and nozzle). These conditions were fixed during the optimization process, in addition to the design variables coming from the main optimization algorithm (see upper left corner of Figure 1). The compressor stagnation pressure ratio was not a design variable, but it was a function of the turbine inlet temperature because, as it increased, the turbine extracted more shaft power to drive the compressor. Therefore, a sub-optimization procedure was implemented within the engine cycle analysis using the golden section method (Press et al. [21]) to maximize the specific thrust with respect to the compressor pressure ratio. The turbine efficiency was also considered to be a function that depended upon a numerical aero-thermal analysis of the hot gas flow through the turbine blade row. That conjugate aero-thermal analysis will be described later. It is understood that the engine cycle analysis (objective function) is strongly affected by the turbine inlet temperature, so Figure 1 shows the inlet temperature as the primary design variable. The process of extracting coolant air from the compressor was also incorporated into the cycle analysis code, affecting both the compressor and turbine efficiencies.

When aerodynamic shape optimization was involved, the external turbine airfoil shape was included in the design variable set coming from the constrained optimization program. The development of the aerodynamic objective function required grid generation in the turbine blade row, as well as a CFD prediction of the hot gas flow-field through the blade row. The aerodynamic objective was quantified by the total pressure loss function, shown as turbine efficiency (Petrovic et al. [22]; Dennis et al. [23]), that was subsequently fed back into the engine cycle analysis (Brown et al. [3]). When the MCADO system operated on a stationary blade such as a guide vane or a stator, this CFD calculation could not provide a measure of the turbine efficiency, and so the aerodynamics did not directly affect the objective function. In those cases, the CFD calculation was executed only once on a fixed blade shape and the objective was strictly a thermal one.

The
that cou
material
coupling
informat
tempera
The bou
a multip
generati
coolant
that carr
the heat
adjusted
design v
entered
converge
heat tra
coolant)

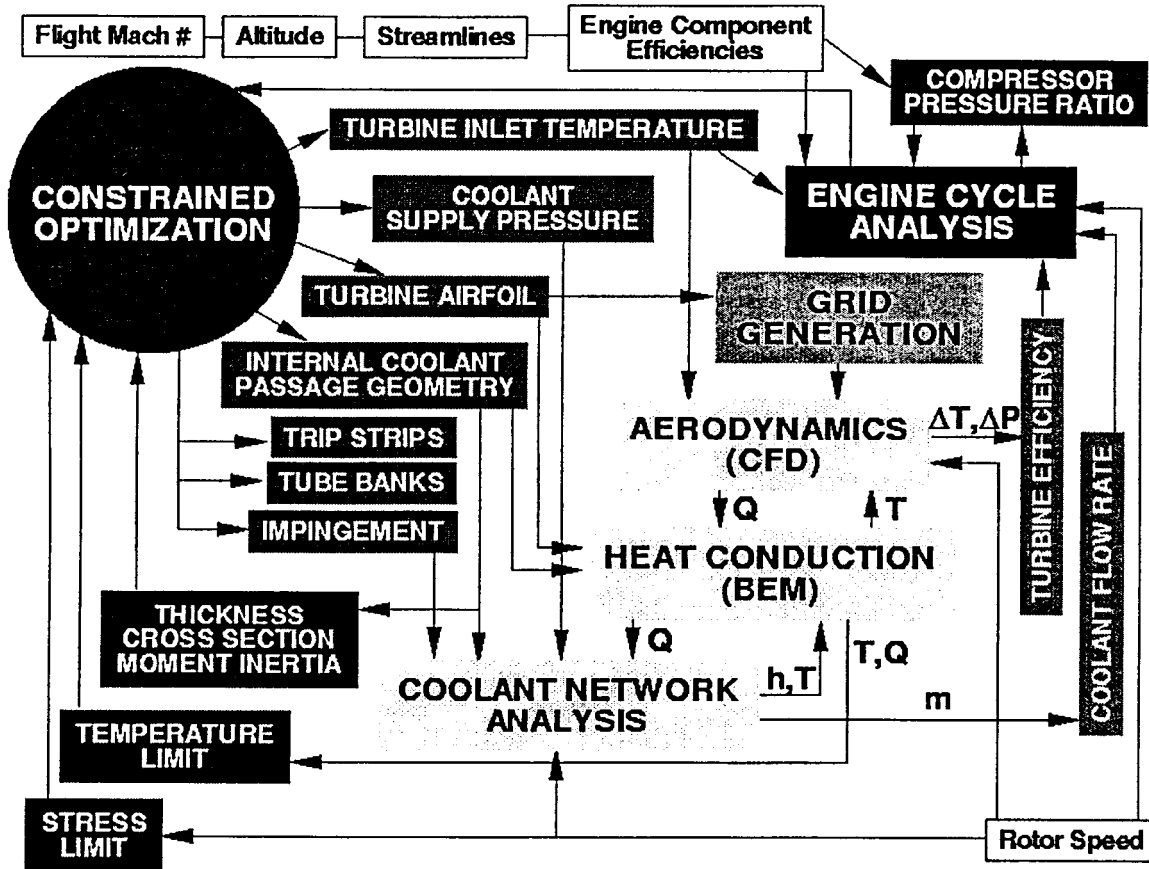


Figure 1: Flow chart for MCADO of internally cooled turbine blades.

The temperature field was determined by a conjugate aero-thermo-fluid numerical analysis that coupled the hot gas flow external to the blade, the heat conduction in the solid blade material and the coolant flow in the internal coolant flow passages. Figure 1 shows an iterative coupling of the three computational components by transferring boundary condition information (temperature T , heat flux Q , heat transfer coefficients h and bulk coolant temperatures, T_c) between them. Any CFD code could be used for the aerodynamic analysis. The boundary element method (BEM) was used to solve the steady heat conduction equation in a multiply coated blade with temperature-dependent material properties. It did not require grid generation inside the blade material. The boundary condition information on the internal coolant passage surfaces existed as heat transfer coefficients and as bulk coolant temperatures that came from a fluid element analysis of an arbitrary coolant network (COOLNET). Since the heat flux into the blade heated the coolant fluid, the bulk coolant temperatures were adjusted during the iterative process. The coolant flow rate and heat transfer enhancement design variables (trip strips and tube banks) from the main constrained optimization program entered into this sub-program. With each iteration, the CFD was executed to partial convergence while the other two components were factored. The overall iterative conjugate heat transfer prediction process among the three components (hot gas, blade material and coolant) completed when the heat flux residual converged.

During the iterative numerical optimization process, the material and structural integrity of the blades was not compromised. The maximum temperature inside the blade was maintained with the enforcement of equality constraint functions and with optimization search directions controlled via projection methods (Foster & Dulikravich [24]). The maximum temperature was a consequence of the coupled CFD/BEM/COOLNET aero-thermo-fluid analysis. A constrained sub-minimization process restored any active or violated constraint functions until a thermally feasible design was reached. Thermal feasibility was defined as a condition when the maximum temperature on the blade surface was less than the melting or limiting oxidation temperature of the blade material. Obviously the performance demands of gas turbine engines must be within the limitations set by the materials used in its construction. Turbine rotor blades are seldom designed to avoid outright failure, but rather to avoid failure within a specified time. Turbine blades are designed to handle four kinds of stresses; centrifugal, bending, vibratory, and thermal. Since we are dealing with a fixed rotor speed and because approximate stress calculations can be justified, a centrifugal stress constraint was enforced by setting a lower limit to the radial cross-sectional area of the blade. Tilting the blade to induce a centrifugal bending in the opposite direction as the pressure load offset the bending stresses. Therefore, given a fixed load, the bending stress constraint was ignored. The thermal stress environment provided an estimate for the mean creep life of the blade, which was subsequently constrained to some minimum life span. Durability limitations caused by steady-state thermo-mechanical fatigue required a two-dimensional thermo-elastic analysis and they were similarly constrained given a number of cycles until failure.

If blade flutter was to be of major concern to the turbine design group, the aero-elastic solution procedure may require a nonlinear dynamic analysis of the blade's structure under transient aerodynamic loads. Full non-linear and time-accurate computational aerodynamics and elasto-dynamics codes are still prohibitively expensive for MCADO. Even reduced-order models are still too expensive, while linearization cannot predict stall flutter, shock-induced oscillations and bending/torsion coupling. A linear dynamic perturbation of a steady aerodynamic analysis may be adequate to resolve transonic shock-induced flutter (Dowell [25]), but even this method is beyond the scope of this research. At the very least, a modal analysis of the blade is necessary to determine its natural vibrational modes. Therefore, aeroelasticity analysis involving fluid-structure interaction will not be addressed here. Instead, simpler structural constraints were used to ensure that the blade's vibrational modes were avoided. Geometric functions such as wall thickness, cross-sectional area and moment of inertia provided an approximate upper limit to maintain structural integrity.

The temperature field (T & Q) computed by the numerical heat conduction analysis (or by a conjugate analysis) was fed one way into a BEM thermo-elasticity algorithm. The BEM was also used for this thermo-elastic analysis because it did not require internal mesh generation. The result of this computation was the thermo-elastic deformation and the thermal stress fields. It has been proven that these displacements (blade deformations) do not significantly affect the resulting heat conduction in the blade. Therefore, the coupling of the heat conduction and thermo-elastic solvers was not iterative.

Objective and constraint information, as well as design sensitivities of those functions with respect to the design variables, were fed back to the main constrained optimization program. The hybrid evolutionary optimization algorithm then determined one or more perturbations to the design variable population, and each required additional objective and constraint function evaluations for the next cycle. The global optimization process proceeded until user-specified tolerances or goals were met. Acceptance of the final design was ultimately the responsibility

of the
have be

1.3 Par

The pa
now be
comple
struts'
variabl
definit
stackin
geomet
outer su

The
of the
determi
followe
edge (F
constan
(Barsky
distance
number

Nex
coordin
defined
one to t
In addit
trailing
modelin
definitic
cutback

The
to devel
generate
impinge
illustrati
the full t

of the cooling systems design engineer who runs the MCADO system, but the repetitive tasks have been left to the computer.

1.3 Parametric model of the turbine airfoil geometry

The parametric model of the internally cooled and thermal barrier coated turbine blade will now be discussed in greater detail. The set of two-dimensional optimization design variables completely defined the shape of the thermal barrier coating, wall thickness variation, internal struts' locations, struts' thicknesses, and their corner fillets. The three-dimensional design variables defined the number of blades in the rotor or stator blade row, the periodic endwall definition for the stream tube, pitch of the leading and trailing edge impingement holes and stacking of sectional airfoil shapes. The turbine airfoils were defined using a conventional geometric definition similar to those used by most industrial turbine design teams. The blade outer surface shape was kept fixed during the internal cooling scheme optimization.

The first step in the development of the multiple coolant flow passages was the description of the cooling wall thickness function. The wall thickness function's ordinate, $W(s)$, determined the thickness of the wall between the hot gas and coolant fluid. The abscissa followed counter-clockwise along the metal/coating interface, s , from trailing edge to trailing edge (Figure 2), where the local coordinate system (x,y) was fixed upon a curved surface at a constant radius from the engine axis. $W(s)$ was defined by a piecewise-continuous β -spline (Barsky [26]) curve that varied in the direction normal to the metal/coating interface to a distance controlled by one design variable per β -spline control vertex. For this research, the number of coolant flow passages in the turbine blade was kept fixed.

Next came the specification of the locations of the internal strut centerlines. The x -coordinates of the intersections of the strut centerlines with the outer turbine airfoil curve were defined as x_{Ssi} and x_{Spi} for the suction and pressure sides, respectively. The index i varied from one to the number of struts, N_{strut} . The range over which each strut could vary was $\pm \Delta x_{Si}$. In addition to the coordinate of the struts, the strut thickness, t_{Si} , and a fillet radius on either the trailing or leading edge sides, e_{Ssi} and e_{Spi} respectively, were used to complete the geometric modeling of each strut. The trailing edge slot is shown on the right hand side of figure 2. The definition of the slot included the slot width, slot length, pressure-side wall thickness and cutback distance.

The virtual geometric parameterization of the turbine airfoil described previously was used to develop two-dimensional sectional geometries. Several other parameters were needed to generate the three-dimensional blade. This included tip cap thickness, tip turn radius, and impingement hole radii and pitches at the leading and trailing edge ribs. Figure 3 is an illustration of a typical thermal barrier coated cored axial turbine blade section on the left and the full three-dimensional stacked blade on the right.

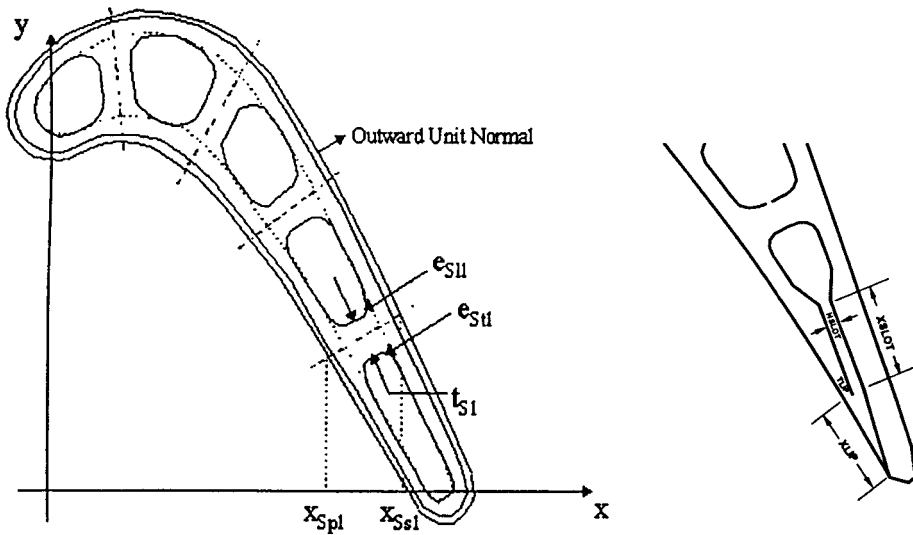


Figure 2: Turbine airfoil, thermal barrier coating and coolant passage geometry. The airfoil contour and coating/metal interface are shown as solid lines. The cooling wall thickness function is used as a reference (dotted line) to draw the coolant passage walls (solid lines).

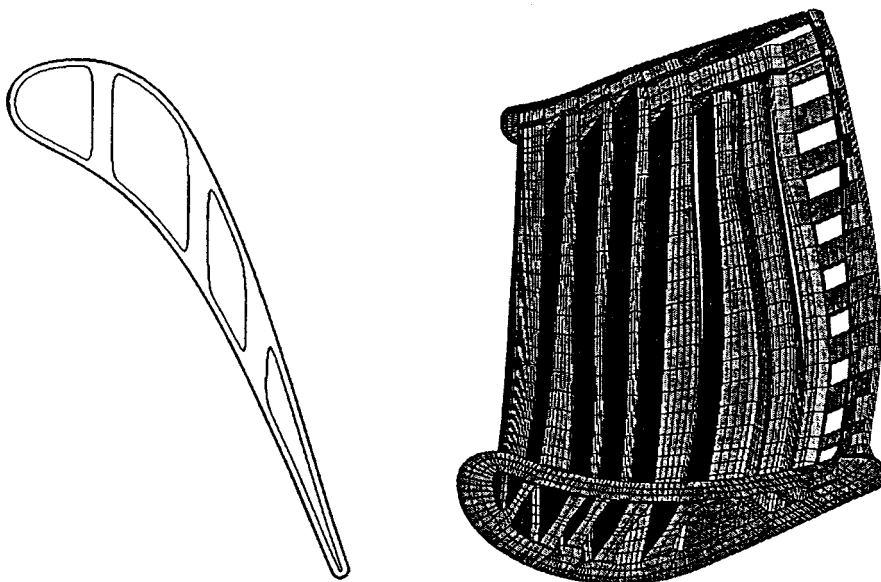


Figure 3: Boundary element discretization of an internally cooled and thermal barrier coated axial gas turbine blade showing the sectional airfoil shapes and a surface mesh.

2 Opt

A cons
FORTH
algorith
each ne
populat
includi
and a
 $H_n(V)$
saved i

This
the Dav
(Goldbe
simulat
optimiz
during
into the
minimiz

The
function
generati
guided
& Dulik
via the
minimiz
feasible

The
to the v
evolved
several
(1) The
(2) The
(3) The
dec
con

2.1 Obj

The prin
that asse
optimiza
different
oxidatio
optimiza

2 Optimization of internally cooled turbine airfoils

A constrained evolutionary hybrid optimization computer program has been developed in the FORTRAN programming language (Martin et al. [16, 20]; Dulikravich et al. [19]). This algorithm creates sequential populations of feasible design variable sets, $\{V\}$, that evolve with each new optimization cycle by minimizing the objective function, $F(V)$, associated with N_{pop} population members. These design variables are subject to a finite number of constraints, including lower and upper bounds on the design variables, $\{V_{\text{min}}\}$ and $\{V_{\text{max}}\}$, respectively, and a finite number of inequality and equality constraint functions, $G_m(V) < 0$ and $H_n(V) = 0$. Only feasible sets of design variables from the current optimization cycle are saved into the population matrix, $[\{V_1\}, \{V_2\}, \dots, \{V_{N_{\text{pop}}}\}]$.

This new hybrid optimization program incorporates four popular optimization algorithms; the Davidon-Fletcher-Powell (DFP) (Davidon [27]) gradient search, a genetic algorithm (GA) (Goldberg [28]), the modified Nelder-Mead (NM) (Nelder & Mead [29]) simplex method, and simulated annealing (SA) (Press et al. [21]). Each technique provides a unique approach to optimization with varying degrees of convergence, reliability and robustness at different cycles during the iterative optimization procedure. A set of rules and switching criteria were coded into the program to switch back and forth among the different algorithms as the iterative minimization process proceeded (Dulikravich et al. [19]).

The evolutionary hybrid scheme handled the existence of equality and inequality constraint functions in three ways: Rosen's projection method, feasible searching and random design generation. Rosen's projection method (Hafka & Gurdal [30]) provided search directions that guided descent-directions tangent to active constraint boundaries. In the feasible search (Foster & Dulikravich [24]), designs that violated constraints were automatically restored to feasibility via the minimization of the active global constraint functions. If at any time this constraint minimization failed, random designs were generated about the current design until a new feasible design was reached.

The population matrix was updated every iteration with new designs, and ranked according to the value of the objective function. As the optimization process proceeded, the population evolved towards the global minimum. The optimization problem was completed when one of several stopping criteria was met:

- (1) The maximum number of iterations or objective function evaluations were exceeded.
- (2) The best design in the population was equivalent to a target design.
- (3) The optimization program tried all four algorithms but failed to produce a non-negligible decrease in the objective function. The latter criterion was the primary qualification of convergence and it usually indicated that a global minimum had been found.

2.1 Objective function formulations

The primary goal of this section is to describe how to establish a quantifiable objective function that assesses the performance and durability of internally cooled configurations for numerical optimization. In order to arrive at the most effective thermal optimization strategy, three different classifications of thermal objective functions have been developed: (1) oxidation/corrosion minimization, (2) coolant effectiveness maximization and (3) engine cycle optimization.

2.1.1 Oxidation/corrosion objective

The oxidation/corrosion minimization strategy made use of an objective that closely resembled one from inverse thermal shape design. At the high temperatures experienced in a turbine, corrosion and oxidation damage affects the life of the airfoil. The addition of thermal barrier coatings and age hardening materials such as chromium and cobalt to the nickel-based turbine blade alloys makes the part resistant to material corrosion. But these materials are expensive, and at the high temperatures experienced by the turbine blades, corrosion still affects the blade life by thinning its walls and weakening the material. Sulfidation is a corrosion phenomenon that results from the condensation of sodium sulfate on the surface of the blade. With increasing surface temperature, the corrosion rate first increases and then decreases because the temperatures are nearer to the vapor pressure of the sodium sulfate and less condensation occurs. In regions where surface temperatures are extremely high, surface atoms react with oxygen and oxidation occurs, and oxidation increases with increasing temperature. Therefore, turbine airfoil life expectancy is at a maximum at a specific temperature, \bar{T} . Therefore, the integrated difference between the computed temperature and user-specified target or mean temperature, \bar{T} , was minimized. The numerical optimization algorithm was used to modify the coolant passage configuration in order to minimize the squared difference between the local computed temperature and the target temperature. The integration was either carried out over the solid domain, Ω .

$$F(V_i) = \int_{\Omega} (T - \bar{T})^2 d\Omega \quad (1)$$

As this function was minimized, the temperature field within the turbine blade approached the desired value and producing a more uniform temperature distribution. The primary outcome of this is the maximization of the oxidation/corrosion life, but it also resulted in a reduction in the thermal stresses. The domain-integrated temperature also had the added advantage of minimizing weight. Unfortunately, it required the resolution of the internal temperature field, a post-processing procedure with the boundary element method, and it requires an internal mesh. Minimization of the boundary-integrated function yielded more uniform temperature fields without the additional difficulties, but the optimization process did not necessarily result in a reduction in weight.

The behavior of this objective was very sensitive to the user-specified target temperature, T . High target temperatures tended to result in lower heat fluxes absorbed by the blade, but they resulted in thicker coolant walls with increased coolant requirements. This tendency was true because the internal surfaces generally have higher heat transfer coefficients and greater surface area exposed to a fluid. Low target temperatures produced less uniform temperature fields because of the maximum temperature equality constraint, thinned the coolant walls and increased the heat flux.

2.1.2 Maximization of the cooling effectiveness

Although the uniform temperature objective did have some desirable features that will be demonstrated later, it has been concluded that it does not consistently satisfy the criterion established for internal turbine coolant passage optimization. With a thermal objective function alone, one can focus only upon one goal. Therefore, we must choose whether we wish to reduce the cooling requirements, improve the airfoil's durability or increase the turbine inlet temperature. The maximization of the cooling effectiveness was tried as one more alternative.

Here T_c
metal te:

In al
blade.
tempera
The opt
because
the resu
leading
increas
perform
function
closed-c

2.1.3 Op
An engin
in order
cooling
importan
thrust (e
specific t

$F(V) =$

Here, in
the turbin
inlet, Q_R
The optim
found by

$$\eta = \frac{T_{\text{cout}} - T_{\text{cin}}}{T_m - T_{\text{cin}}} \quad (2)$$

Here T_{cin} is the bulk coolant temperature at the inlet to the coolant passages, T_m is the blade metal temperature and T_g is the hot gas temperature.

In all cases studied, the maximum cooling effectiveness increased the heat flux into the blade. The internal heat transfer coefficients were increased to their upper limit, the bulk temperatures of the coolant became higher and the coolant walls became as thin as possible. The optimized design dramatically increased the pressure losses in the coolant passages, because the objective favored high heat transfer coefficients. This increased heat transfer was the result of increased wall roughness and there were large increases in the heat flux at the leading and trailing edges. Heat flux maximization did have some favorable consequences by increasing the turbine inlet temperature, but it provided no information about the engine performance loss caused by the bleeding of air from the compressor. It is a viable objective function only if it is decoupled from the aerodynamic and overall engine performance for closed-circuit cooling devices, for example.

2.1.3 Optimization of the engine cycle

An engine cycle analysis was implemented as a more realistic optimization objective function in order to take into account the effects of aerodynamic losses, fuel economy and internal cooling losses simultaneously with an increase in the turbine inlet temperature. One of two important performance parameters of a gas turbine engine will be optimized, either specific thrust (engine thrust force per linear momentum of engine air flow rate, $\mathfrak{S}/\dot{m}v_\infty$), or thrust specific fuel consumption (mass flow rate of fuel per unit thrust, \dot{m}_f/\mathfrak{S}). (Kerrebrock [31]).

$$F(V) = \frac{\mathfrak{S}}{\dot{m}v_\infty} = \sqrt{\left(\frac{T_{01}/T_1}{T_{01}/T_1 - 1}\right) \left(\frac{T_{0t}/T_1}{(T_{01}/T_1)\pi_c^{1-\frac{1}{\gamma}} - 1}\right) \left(\pi_c^{1-\frac{1}{\gamma}} - 1\right) + \frac{T_{0t}/T_1}{(T_{01}/T_1)\pi_c^{1-\frac{1}{\gamma}} - 1} - 1} \quad (3)$$

$$F(V) = \frac{\dot{m}_f}{\mathfrak{S}} = \frac{c_p \left(T_{0t}/T_1 - (T_{01}/T_1)\pi_c^{1-\frac{1}{\gamma}}\right)}{Q_R \left(\frac{\mathfrak{S}}{\dot{m}}\right)} \quad (4)$$

Here, \dot{m} is the air mass flow rate, \dot{m}_f is the fuel mass flow rate, v_∞ is the flight speed, T_{0t} is the turbine inlet total temperature, T_{01} and T_1 are the total and static temperatures at the engine inlet, Q_R is the heat value of the fuel, and π_c is the compressor stagnation pressure rise ratio. The optimum compressor pressure ratio for an ideal turbojet at maximum specific thrust can be found by differentiating specific thrust with respect to the compressor ratio [1].

